

# MINC: A MINIATURE INTEGRATED GUIDANCE, NAVIGATION & CONTROL SYSTEM ENABLES IN-FLIGHT GPS/INS DATA FUSION ABOARD A MICRO AERIAL VEHICLE

**Marco Buschmann, Axel Heindorf, Stefan Winkler, Peter Vörsmann  
Institute of Aerospace Systems, Technical University of Braunschweig, Germany**

## Abstract

*The Institute of Aerospace Systems of the Technical University of Braunschweig has developed a highly miniaturized yet powerful Miniature Integrated Navigation and Control (MINC) system allowing for highly dynamic on-board flight control using a tightly coupled Kalman filter for GPS/INS data fusion. The whole system with all micro-electromechanical (MEMS) sensors measures 40 x 80 x 15 mm<sup>3</sup> at a mass of only 20 grams.*

## 1 Introduction

The interest in small Unmanned Aerial Vehicles (UAV) and Micro Aerial Vehicles (MAV) is steadily increasing during the last years [1] [2], mainly driven by the promising applications such systems allow. However, the usefulness of such devices is directly coupled to their grade of autonomy in flight.

Since 2001, the Institute of Aerospace Systems (ILR) of the Technical University of Braunschweig, Germany, is working on autonomous Mini and Micro Aerial Vehicles (MAV) [3]. Emphasis is put on a high degree of on-board autonomy: The aircraft shall be able of guidance, navigation, and control without requiring intervention from the user on ground. Main focus of the recent developments is a precise and reliable attitude determination, the basis for highly dynamic flight control. This paper will deepen on the hardware development, both for attitude determination and flight control, of the current autopilot hardware.

## 1.1 The Project “Carolo”

During the project “Carolo” (2003 to 2006), the first MAV-prototype “Carolo P50” was developed: a miniature drone with 50 cm wingspan and a take-off mass of approximately 500 g, capable of automatic start, waypoint navigation and landing, with the first automatic flight taking place in 2004 [4].



Fig. 1: Prototype “Carolo P50”

For this family of MAV and Mini-UAV, a special “Carolo” autopilot system was developed, based on micro-electromechanical (MEMS) inertial sensors and MEMS-sensors for static and impact pressure. This type of sensors is known for their poor performance regarding accuracy, long-term stability and temperature dependency, but this class of sensors is the only one which fulfills the stringent requirements regarding size, weight and power consumption aboard a MAV.

The flight guidance and control algorithms of the Carolo autopilot were hosted on a 32 bit CPU running at 200 MHz. Navigation was done using the GPS satellite navigation system, but no GPS/INS data fusion algorithms were applied, keeping the computing demands low, but causing reliability problems on the smallest prototype P50 at gusty wind or flight trajectories requiring highly dynamic flight control.

## 1.2 The Project “AutoMAV”

Since 2004, several leading research institutions in Germany are jointly working on a new MAV project called “AutoMAV” within the German National Aerospace Program 2003-2007 [5]. Besides the Institute of Aerospace Systems as project head, the Institute of Flight Guidance, the Institute of Aircraft Design and Lightweight Structures and the Institute of Fluid Mechanics of the Technical University of Braunschweig are involved, as well as the Chair of Flight Dynamics of the RWTH Aachen and the DLR Institute of Aeroelasticity, Göttingen, are contributing their expertise to develop a fully autonomous MAV with a wing span of 38 cm and a take-off mass of 400 g. The payload of the electrically propelled AutoMAV consists of a small video camera with an analog downlink.

As can be seen in Fig. 2, the AutoMAV shows a rather unconventional ‘twin-wing’ configuration: The main body reminds of a delta-shaped flying wing with a thick airfoil to accommodate the aircraft subsystems, as commonly used for MAVs. But in this case, the aircraft also uses an elevator for longitudinal control, which is mounted beneath the main wing to ensure sufficient controllability even at near-stall angles of attack.

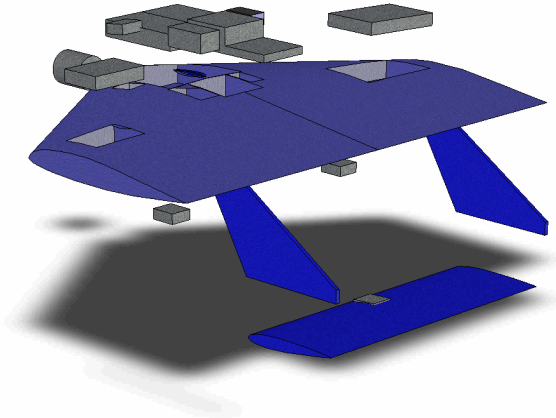


Fig. 2: The MAV of the AutoMAV Project

Current flight control systems for Mini-UAV and MAV usually use simple (and computationally undemanding) flight control algorithms, usually resulting in well-damped (and hence controllable), but not agile aircraft. One goal of the AutoMAV project was to redefine flight performance for small MAVs: The aircraft shall be able to perform highly accurate and dynamic flight control even under bad circumstances like gusts and shall allow for demanding flight trajectories with sharp turns and high bank angles, thus using the aerodynamic and flightmechanical potential of this class of aircraft to its full extent. To achieve this performance only with MEMS-based inertial sensors and a satellite navigation system, on-board data fusion of GPS and INS data is essential.

## 2 The Miniature Integrated Navigation and Control System

An autopilot, on its basic level, generally has the task of determining the aircraft current state, compare it with the desired state and drive the control surfaces in such a way that the desired state is achieved. For control surface actuation commercially available products from the model plane market fulfill most MAV requirements; the main challenge is the aircraft state determination. Hence, the field of classical flight control and flight guidance as in [6] shall not be subject of this paper, but emphasis shall be put on aircraft state determination.

The development of the AutoMAV flight control hardware was driven by the demand for sophisticated on-board GPS/INS data fusion to overcome the shortcomings of MEMS-based inertial navigation. A plain and commonly used approach to avoid high computational load aboard the aircraft is to send sensor data down to ground control, process all data on a conventional PC, and send the control surface commands back to the aircraft. However, this concept obviously is in opposition to the demand for autonomous flight, since it would require a permanent and reliable radio connection between aircraft and ground control.

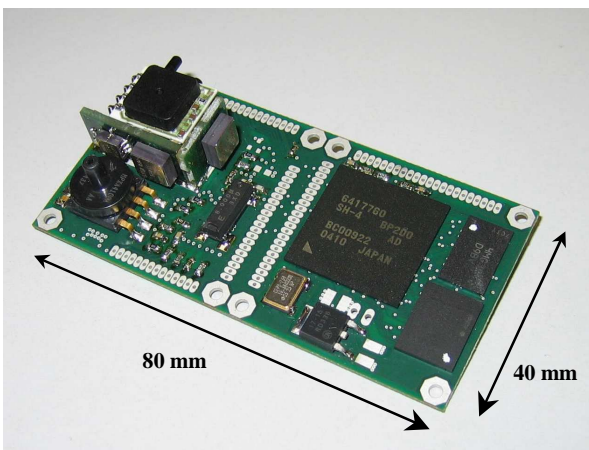


Fig. 3: The MINC System

The answer to the unusually risen demand for computational power aboard a MAV is a completely new autopilot hardware called Miniature Integrated Navigation and Control

(MINC) System (Fig. 3), measuring only  $40 \times 80 \times 15 \text{ mm}^3$  at a mass of 20 g (without connectors and GPS receiver).

As a successor of the “Carolo” autopilot, the MINC System incorporates several MEMS-based sensors to form a complete 3-axis IMU as well as sensors for barometric altitude and flight speed determination, with a data acquisition rate of 100 Hz. It also provides outputs for servo actuator control, matching the sensor sampling frequency and allowing a closed loop control frequency of true 100 Hz.

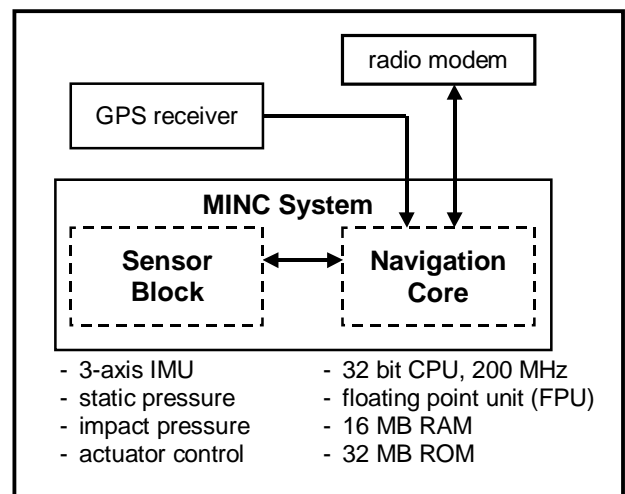


Fig. 4: MINC System, Block Diagram

The simplified block diagram of the system is shown in Fig. 4. As can be seen, it consists mainly of two functionally separated blocks, communicating via a bidirectional data link: Sensor Block and Navigation Core. The following sections further describe these blocks in more detail.

### 2.1 The MINC Sensor Block

The Sensor Block is located in the left part of the MINC System (according to Fig. 3), and geometrically and electrically forms a self contained unit; for evaluation the Sensor Block was built up as a separate board, measuring  $40 \times 40 \times 15 \text{ mm}^3$  and weighting 15 grams. The block diagram of the Sensor Block is shown in Fig. 5.

### 2.1.1 Sensor Block Structure

Central part of the Sensor Block is a microcontroller, which communicates with the Navigation Core via a digital serial link and several control lines for time synchronization. For analog data acquisition, the block contains all necessary A/D converters.

The Sensor Block has two main functions: First, as the name suggests, it contains all sensors for inertial measurement, forming a complete 6-degree-of-freedom IMU. In addition, the temperatures of the single-axis

angular rate sensors are measured individually to allow for temperature calibration. Sampling resolution is 12 bit with a nominal sampling rate of 100 Hz. The linear accelerations are measured using 2-axis sensors, thus giving a redundancy for the x-axis. The impact pressure is also captured using 12 bit resolution, but for the static pressure, a high-resolution sigma-delta A/D converter is used, resulting in a relative accuracy (not considering drift and temperature effects) of better than 30 cm near sea level.

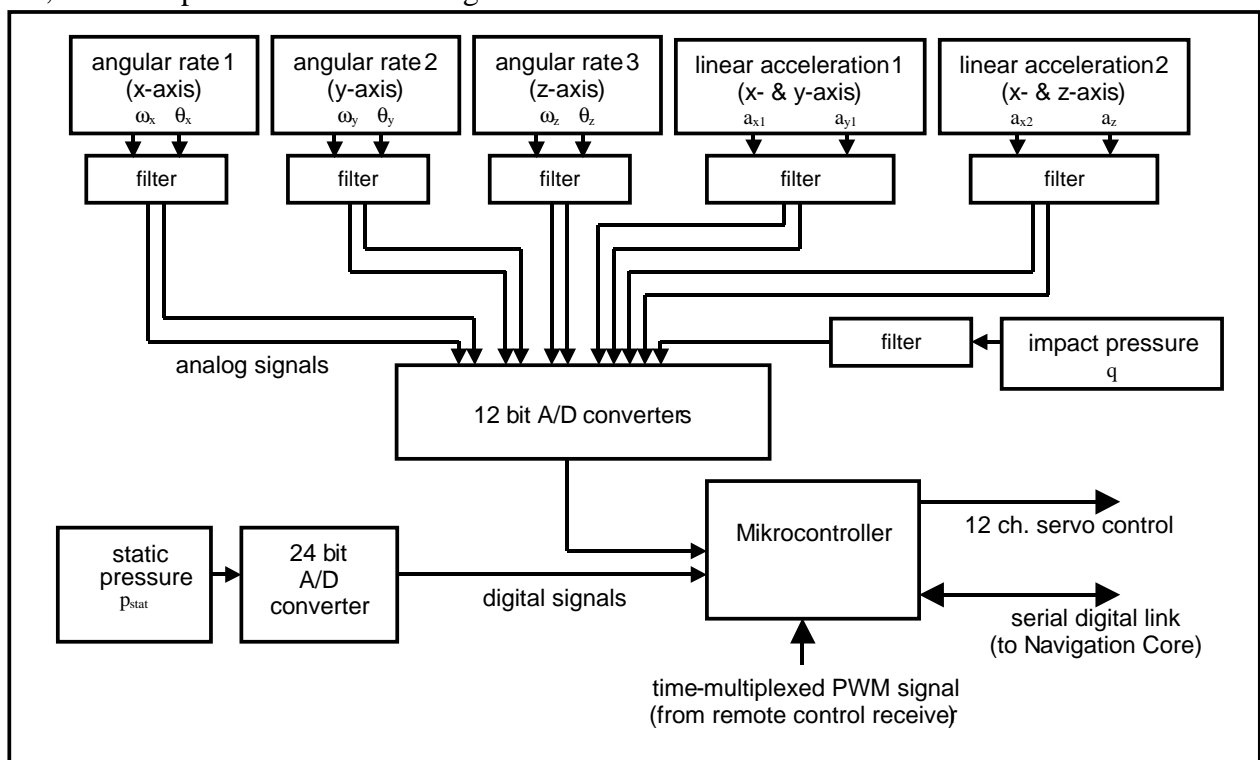


Fig. 5: Block Diagram of the MINC Sensor Block

The second main function is the generation of pulsewidth-modulated (PWM) signals for servo actuator control. The Sensor Block is capable of generating 12 independent PWM outputs with a period of 100 Hz and a pulse width resolution of 1  $\mu$ s. Since the generation of these signals completely occurs in the digital domain, this task is comparably easy, bearing few distress of signal noise or distortion. Full characteristics of the Sensor Block are listed in Tab. 1.

In addition to these two primary functions, the Sensor Block also contains an input for a time-multiplexed signal from a common remote

control receiver, as widely used in remote-controlled model planes. This adds an important safety feature to the MINC System: The aircraft can be controlled via the Sensor Block directly from the ground using a model plane remote control. This is possible without passing data through the Navigation Core, giving a real back-up control possibility in case of severe malfunction of the Navigation Core hard- or software, which especially eases the development, on-board implementation and performance testing of the navigation and control algorithms.

<b>sensors</b>	<b>measurement range</b>
angular rates (x-, y- & z-axis)	$\pm 300$ °/s $\approx \pm 5.2$ rad/s
lin. acceleration (x- & y-axis)	$\pm 15$ m/s <sup>2</sup> $\approx \pm 1.5$ g
lin. acceleration (x- & z-axis)	$\pm 80$ m/s <sup>2</sup> $\approx \pm 8.2$ g
static pressure	15 to 105 kPa
impact pressure	0 to 1.250 Pa
<b>derived air data<sup>1</sup></b>	<b>measurement range</b>
barometric altitude	0 to 13 km
air speed	0 to 45 m/s (h = 0 km) 0 to 91 m/s (h = 13 km)
<b>additional functionality</b>	
actuator control (PWM)	12 ch., 100 Hz period
remote control input	1 channel, time-muxed

Tab. 1: Sensor Block Characteristics

### 2.1.2 Data Quality

Within the MINC System, analog and digital electronic components are integrated with a high packing density. Besides this, the stringent constraints regarding size do not allow for high order analog filtering of sensor signals, as would be good design practice under normal circumstances. To ensure sensor data quality and integrity, the first prototypes were subject to intensive testing. This was partly done at the Institute of Flight Systems, DLR Braunschweig, using a precision turn table and climate chambers. As an exemplary result, a time series of a z-axis angular rate sensors (A/D converter digits over time) is shown in Fig. 6, together with the autocovariance and the power spectrum of the dataset. As can be seen, the peak-to-peak noise is approximately 8 digits, corresponding to approximately 2 °/s.

The autocovariance shows very low self-similarity; no signs of unwanted oscillations or beats can be observed. The overall signal quality can be considered quite good for such a highly integrated MEMS sensor system, showing an approximation to white noise, which is important for the GPS/INS integration filter.

### 2.1.3 Sensor Calibration

To overcome the well-known problem of temperature dependency of MEMS-based sensors, several Sensor Block prototypes were calibrated at temperatures from  $-20$  °C to  $+50$  °C using a climate chamber. But besides temperature effects, also misalignment plays an important role. Especially since the Sensor Block prototypes were manually assembled, misalignment errors of up to 10% can easily occur.

Basically, the sensor set of gyros and accelerometers form a coordinate system with e.g.  $\overline{\omega}_S = (\omega_{x,S} \ \omega_{y,S} \ \omega_{z,S})$  being the angular rate vector measured by the three gyros (index  $x$ ,  $y$ , and  $z$ ) in the sensor-fixed coordinate system (index  $S$ ). The unit of this vector is plain *digits* as given by the A/D converter, not containing any scaling to physical units (e.g. °/s). Please note, that the axes  $x$ ,  $y$ , and  $z$  do not form an orthogonal or even right-handed coordinate system.

Similarly, the accelerometers deliver four accelerations  $a_{x1,S}$ ,  $a_{y,S}$ ,  $a_{z,S}$ ,  $a_{x2,S}$  (with redundancy for the  $x$ -axis), but for clarification, only the angular rates are being considered in the following steps, the process is analog for the linear accelerations.

To obtain the desired angular rate vector  $\overline{\omega}_g = (\omega_{x,g} \ \omega_{y,g} \ \omega_{z,g})$  in the geometric coordinate system (index  $g$ , not to be confused with the geodetic system), the following transformation (Eq. 1 and 2) can be used to transform the measured angular rates  $\overline{\omega}_S$  using a transformation matrix  $M$ . The coefficients  $k_{i,j}$  of the transformation matrix  $M$  describe the contribution of the sensor  $i$  to the desired value along the geometric axis  $j$ . The coefficients  $k_{i,j}$  contain not only the misalignment correction, but also the (temperature-dependent) scale factor for each sensor. So strictly speaking,  $M$  is a function of the Temperature  $T$ . Besides this, the individual, temperature-dependent bias  $b_i$  (in digits) of each sensor has to be known.

<sup>1</sup> assuming ICAO standard atmosphere

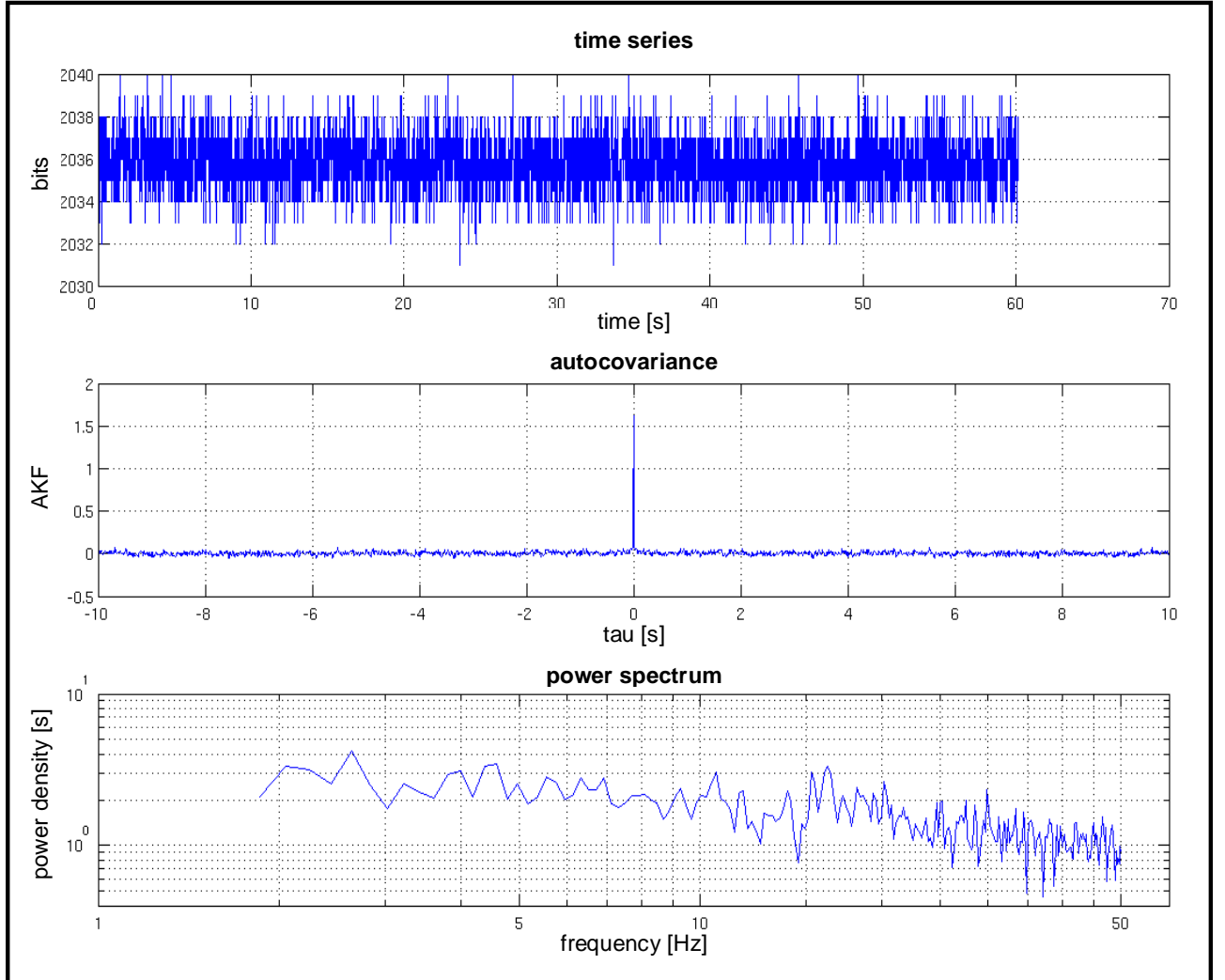


Fig. 6: Exemplary Raw Data Time Series of a z-Axis Angular Rate Sensor, together with the corresponding Autocovariance (AKF) and Power Spectrum

$$\overline{\omega}_g = M(T) \cdot (\overline{\omega}_s - \overline{b(T)}) \quad (1)$$

$$\begin{pmatrix} \omega_{x,g} \\ \omega_{y,g} \\ \omega_{z,g} \end{pmatrix} = \begin{pmatrix} k_{x,x} & k_{y,x} & k_{z,x} \\ k_{x,y} & k_{y,y} & k_{z,y} \\ k_{x,z} & k_{y,z} & k_{z,z} \end{pmatrix} \cdot \begin{pmatrix} \omega_{x,S} - b_x \\ \omega_{y,S} - b_y \\ \omega_{z,S} - b_z \end{pmatrix} \quad (2)$$

Unfortunately, the Sensor Blocks had to be statically mounted within the climate chamber, prohibiting dynamic measurements at different temperatures. So for the angular rates, only the bias could be determined as function of temperature, the change of scale factors within

the transformation matrix could not be observed. However, for one temperature (room temperature), each geometric Sensor Block axis was calibrated for angular rates of  $\pm 300$  °/s in steps of 50 °/s, using a precision turn table. Besides linearity investigations, these measurements reveal the cross-axis sensitivity due to the sensor misalignment and led to the determination of the matrix  $M$ , which then had to be considered temperature-independent.

Due to gravity, at least one axis of the accelerometers is always excited. To distinguish temperature dependency of bias and scale for the accelerometers, several measurements were conducted over a temperature range from  $-20$  °C to  $+50$  °C with different Sensor Block placements, allowing for bias determination

over temperature, and in this case also scale (and misalignment) over temperature.

The temperature-dependent coefficients for sensor bias can be easily approximated with sufficient accuracy within the Sensor Block using the integrated microcontroller, which also transforms the measured angular rates and linear accelerations according to the stored temperature-invariant transformation matrices. As a result, the Sensor Block can directly deliver calibrated measurements in physical units to the Navigation Core.

## 2.2 The MINC Navigation Core

The Navigation Core, as the Sensor Block, forms a geometrically and electrically separated unit measuring 40 x 40 x 6 mm<sup>3</sup>. It mainly consists of a powerful 32 bit CPU and hosts the main guidance, navigation and control algorithms.

### 2.2.1 Navigation Core Hardware

While simple control algorithms can be easily realized with fixed-point arithmetics, the implementation of more and more complex algorithms is increasingly calling for floating point arithmetics, and in the case of INS/GPS data fusion, even the use of double precision (64 bit) numbers can be necessary. It shall be noted, however, that every algorithm can be implemented using fixed point arithmetics only, but even with convenient tools and powerful programming extensions like “System C”, the use of fixed point arithmetics is still a time-consuming process which holds lots of pitfalls for the code developer during algorithm implementation and verification.

These considerations, together with the requirements for low power consumption and small footprint, led to the choice of a 32 bit CPU running at 200 MHz. The main criterion for choosing this CPU type was its integrated Floating Point Unit (FPU), which allows for addition, multiplication and division of floating point numbers with single (32 bit) and double precision (64 bit) in hardware.

Fig. 7 shows a comparison between the ILR’s 1<sup>st</sup> generation Carolo Autopilot module,

using only integer arithmetics, and the 2<sup>nd</sup> generation MINC System. While the old system emulated all floating point operations by using 32 bit integer arithmetics, the MINC System utilizes its built-in FPU.

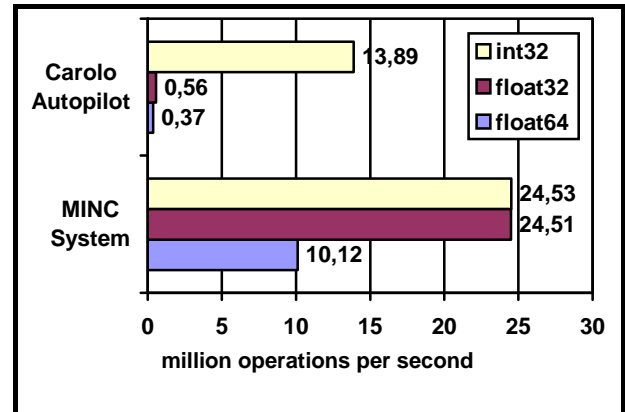


Fig. 7: Comparison of Carolo Autopilot and MINC System

The comparison data was derived by running an addition and multiplication test loop. Shown are the achieved million operations per second, where “one operation” refers to one loop pass with alternately one addition or one multiplication. The operations were done within a large data array to force external memory accesses and prevent the exclusive use of internal registers. However, both instruction and data caching for both platforms was enabled, allowing for efficient memory burst accesses.

The test loops were run for integer arithmetics with 32 bit precision (labeled int32) and floating-point arithmetics with both single (float32) and double precision (float64). As can be seen, the old design is outperformed up to twentyfold by the new design for floating point arithmetics.

The Navigation Core is powered by a single, regulated 3.3 V supply, the average power consumption during test loop load was approximately 0.9 watt, being reasonable for the use within a MAV.

Besides the FPU, the Navigation Core provides several interfaces for connecting to the Sensor Block the external miniaturized GPS receiver and an optional radio modem for communication with ground control. In addition, a MultiMediaCard can be directly connected as mass-storage device for in-flight data recording. Provision is made to connect other periphery via USB<sup>2</sup> or CAN<sup>3</sup> bus in the future.

### 2.2.2 Navigation Filter

For GPS/INS integration, a discrete error state Kalman Filter of state vector  $\mathbf{x}$  (Eq. 3) was used [7]. By processing measurements from one single-antenna stand-alone GPS receiver, it provides estimates for the three position, three velocity and three attitude errors as well as the three errors in the gyro sensor signal bias estimates, the three errors in the accelerometer signal bias estimates, the error in the GPS receiver (RX) clock error and the error in the GPS RX clock drift (17 states). The calculating time for one propagation step of this type of Kalman filter on the MINC Navigation Core is approximately 1 ms, easily matching the sensor and actuator update frequency of 100 Hz while providing enough spare capability for the 1 Hz filter update, flight controller and flight guidance (not subject of this paper) and supplementary tasks like protocol handling for communication with ground control.

$$\mathbf{x} = \begin{bmatrix} \delta\mathbf{r} & \dots & \text{position error} \\ \delta\mathbf{v} & \dots & \text{velocity error} \\ \delta\boldsymbol{\varphi} & \dots & \text{attitude error} \\ \delta\boldsymbol{\omega} & \dots & \text{error of est. gyro signal bias} \\ \delta\mathbf{a} & \dots & \text{error of est. acc. signal bias} \\ \delta(c\Delta t) & \dots & \text{error of RX clock error} \\ \delta(c\Delta\dot{t}) & \dots & \text{error of RX clock drift} \end{bmatrix} \quad (3)$$

As aiding information, GPS raw data were used in order to closely meet the Kalman Filter requirement of zero-mean and uncorrelated white measurement noise (tightly-coupled). Furthermore, with such a filter the IMU can still

be aided by GPS when there are less than 4 satellites in the field of view of the GPS antenna. These two significant features can not be fulfilled by using the position and velocity outputs of the GPS receiver directly (loosely-coupled).

Often, the measurement vector  $\mathbf{z}$  of a tightly-coupled Kalman Filter contains ranges and delta-ranges. But in the filter used here the delta-ranges were replaced by time-differenced carrier phases. The key idea of this method is to improve the velocity aiding and hence the attitude estimate of the filter which is the most important aircraft state in order to achieve good flight performances of autonomous MAVs.

### 2.3.2 Flight Test Results

A GN&C test platform was developed by the institute. It is a small UAV of 2 m wing span and about 5 kg maximum take-off weight, while offering 1.8 kg of payload capacity. For the flight test the GN&C test platform was equipped with both a reference navigation system (integrated FOG-IMU/GPS) and the MINC System.

The accuracy of the low-cost navigation system is given with respect to the reference navigation system. The error of roll angle  $\Phi$ , pitch angle  $\Theta$  and yaw angle  $\Psi$  using the 17 state Kalman filter with state vector from Eq. (3) is shown in Fig. 8. As expected, roll and pitch angle show a little better accuracy than yaw angle due to gravity influence. Fig. 9 shows the corresponding roll angle for this flight leg as well as the number of tracked satellites, which decreases temporarily at high roll angles. The attitude accuracies ( $1\sigma$ ) for roll, pitch and yaw are listed in Tab. 2.

attitude error ( $1\sigma$ )	17 state Kalman Filter
roll angle	0.76 °
pitch angle	0.75 °
yaw angle	1.50 °

Tab. 2: Attitude Errors of the MINC System

<sup>2</sup> USB: Universal Serial Bus

<sup>3</sup> CAN: Controller Area Network



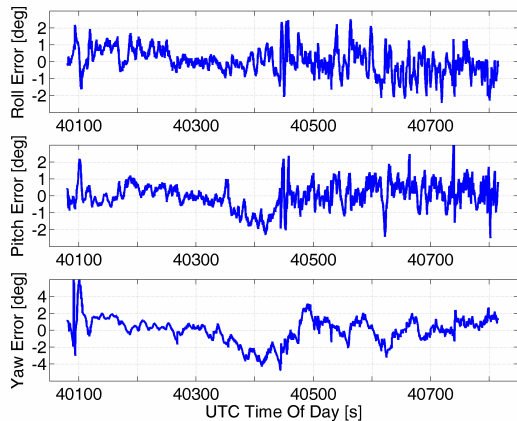


Fig. 8: Attitude Errors of the MINC System

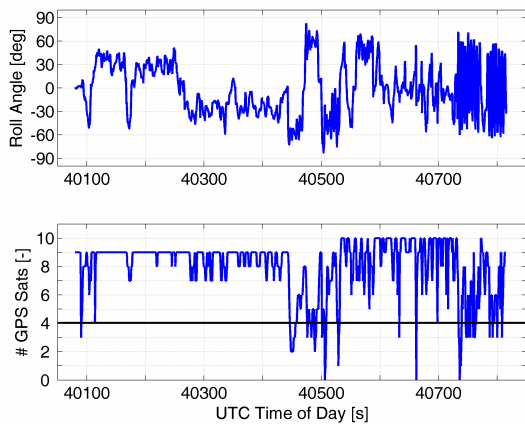


Fig. 9: Roll Angle and Number of Satellites tracked during Flight Test

### 3 Summary and Outlook

At the institute of Aerospace Systems, a highly miniaturized, yet powerful autopilot system for MAV and Mini-UAV was developed. The system includes a 6-DOF-IMU based on MEMS sensors, which was calibrated regarding temperature dependency and sensor misalignment.

Contrary to other currently available autopilot systems for MAV, the MINC System contains a powerful CPU with integrating Floating Point Unit, significantly accelerating floating point operations at single (32 bit) and double precision (64 bit).

Besides the classical flight control and flight guidance, this allows for demanding GPS/INS data fusion algorithms in real-time, allowing highly dynamic autonomous flight.

The currently implemented navigation filter consists of a tightly-coupled Kalman filter with 17 states, delivering GPS-aided aircraft position, velocity and attitude at 100 Hz.

The MINC System (without GPS receiver) measures  $80 \times 40 \times 15 \text{ mm}^3$  at a mass of only 20 grams.

### Acknowledgements

The authors wish to thank the German Government for financing the project AutoMAV within the German National Aerospace Program 2003-2007, and the DLR Institute of Flight Systems, Braunschweig, for providing the facilities necessary for IMU calibration.

### References

- [1] Grasmeyer J M and Keennon M. Development of the Black Widow micro air vehicle. *AIAA 39th Aerospace Sciences Meeting and Exhibit*, Reno, NV, Jan. 8-11, 2001
- [2] Wu H, Sun D and Zhou. Micro Air Vehicle: Configuration, Analysis, Fabrication, and Test, *IEEE/ASME Transactions on Mechatronics*, vol. 9, no. 1, p. 108-117, march 2004
- [3] Kordes T, Buschmann M, Schulz H-W, Vörsmann P. Progresses in the Development of the Fully Autonomous MAV CAROLO. *Proceedings of 2nd AIAA "Unmanned Unlimited"*, San Diego, California, September 2003
- [4] Schulz H-W, Buschmann M, Kordes T, Krüger L, Winkler S, Vörsmann P. The Autonomous Micro and Mini UAVs of the Carolo-Family. *Proceedings of the AIAA Infotech@Aerospace*, Arlington, Virginia, American Institute of Aeronautics and Astronautics, AIAA-2005-7092, 2005
- [5] Winkler S, Buschmann M, Krüger L, Schulz H-W, Vörsmann P, Ronnenberg A, Hecker P, Hansen L, Horst P, Möller T, Wokoeck R, Radespiel R, Nowack J, Alles W, Wegner W. AutoMAV – Überwachung mit autonomen Mikroflugzeuge im deutschen Luftfahrtforschungsprogramm 2003-2007: Überblick und aktuelle Ergebnisse. *Jahrbuch 2005 der Deutschen Gesellschaft für Luft- und Raumfahrt*, Bonn, Deutsche Gesellschaft für Luft- und Raumfahrt, 2005
- [6] Brockhaus R, *Flugregelung*, ISBN 3-540-41890-3, Springer Verlag, 2002,
- [7] Gelb, A.: *Applied Optimal Estimation*. 11th Printing. Cambridge, MA, London : The M.I.T. Press, 1989